

IPTC 10660

Information content in forward 4D seismic modelling and elastic inversion

A. Skorstad, Norwegian Computing Center; O. Kolbjørnsen, Norwegian Computing Center; Å. Drottning, NORSAR; H. Gjølsetdal, NORSAR; and O. Huseby, Institute for Energy Technology

Copyright 2005, International Petroleum Technology Conference

This paper was prepared for presentation at the International Petroleum Technology Conference held in Doha, Qatar, 21–23 November 2005.

This paper was selected for presentation by an IPTC Programme Committee following review of information contained in a proposal submitted by the author(s). Contents of the paper, as presented, have not been reviewed by the International Petroleum Technology Conference and are subject to correction by the author(s). The material, as presented, does not necessarily reflect any position of the International Petroleum Technology Conference, its officers, or members. Papers presented at IPTC are subject to publication review by Sponsor Society Committees of IPTC. Electronic reproduction, distribution, or storage of any part of this paper for commercial purposes without the written consent of the International Petroleum Technology Conference is prohibited. Permission to reproduce in print is restricted to an abstract of not more than 300 words; illustrations may not be copied. The abstract must contain conspicuous acknowledgment of where and by whom the paper was presented. Write Librarian, IPTC, P.O. Box 833836, Richardson, TX 75083-3836, U.S.A., fax 01-972-952-9435.

Abstract

Elastic seismic inversion is a tool frequently used in analysis of seismic data. Elastic inversion relies on a simplified seismic model, and generally produces 3D cubes for V_p , V_s and density. By applying rock physics theory such volumes may be interpreted in terms of lithology and fluid properties. Understanding the robustness of forward and inverse techniques is important when deciding how much information seismic data really carry.

This paper discusses the observed deviation between a reference and simulated reservoir, and its dependency on the seismic parameters and the reservoir characterization parameters. The ability to utilize the results from a 4D seismic survey in reservoir characterization will depend on several aspects. To investigate this, a loop that performs independent forward seismic modeling and elastic inversion at two time stages has been established.

The multi-disciplinary workflow has several independent steps:

1. Generation of a synthetic reference reservoir, by realistic geostatistical modeling.
2. Flow simulation of the reference reservoir to predict reservoir conditions at survey acquisition times.
3. Establishing a relationship between petrophysical and fluid properties and seismic parameters by a rock physics model.
4. Generation of seismic AVA responses corresponding to reservoir conditions at base and monitor survey times.
5. Elastic seismic inversion of both AVA response sets.
6. Simulation of lithology and fluid parameters conditioned on seismic inversion.
7. Comparison of static reservoir parameters of reference and simulated realization.

8. Comparison of seismic responses at initial and monitor survey times.

By working on a realistic synthetic reservoir, full knowledge of the reservoir characteristics is achieved. This makes the evaluation of the questions regarding the fundamental dependency between the seismic and petrophysical domains stronger. The theoretical limitations of the information content of the seismic data, including 4D, are investigated since the synthetic reservoir is an ideal case with accuracy never achieved in the applied situation.

The production deviation between the reference and predicted reservoir was significantly decreased by using 4D seismic data in addition to the 3D inverted elastic parameters.

Introduction

It is well known that the information in seismic data limited by the band width of the seismic signal. 4D seismic give information of the changes between base and monitor survey, and will thereby be an important source of information regarding the principal flow in the reservoir. Due to its limited resolution, the presence of a thin thief-zone can only be observed as a consequence of flow, and the exact location will not be directly found. This paper addresses the question on how much information content there is in the seismic data, and how this information can be used to update the initial distribution of petrophysical reservoir parameters.

A workflow was defined to generate realistic data at various levels including seismic amplitudes, inverted elastic and petrophysical parameters as well as the flow domain.

The initial reservoir was a realistic synthetic elastic reservoir penetrated by eight vertical wells. A full reservoir simulation was run followed by a forward seismic modeling. Elastic parameters were generated by an inversion on the pre-production seismic amplitudes, using different rock physics assumptions. These were used to condition a prediction of the petrophysical reservoir parameters. This prediction represents the average of typical guesses (stochastic realizations) of the reservoir at the pre-production phase. Running flow simulations on such realizations give flow rates that in general will deviate from the true flow behavior. Elastic parameters from an inversion of the monitor survey seismic amplitudes will be updated reflecting the changes in the reservoir. This paper investigates whether the inclusion of these updated elastic parameters gives added value such that the stochastic realizations of the petrophysical properties can be better determined, with special focus on the thief zone.

Synthetic reservoir

The rationale behind using a synthetic reservoir was to have full control on the true reservoir. This enables more accurate and quantitative comparisons with the generated realizations. Although the reservoir is synthetic, it is important to incorporate realistic behavior in it. The synthetic reservoir is based on two synthetic reservoirs from the European Union research project SAIGUP (Skorstad et al., 2005). Here, considerable effort was made in generating realistic synthetic reservoirs based on observed features in both recent and ancient shallow marine systems. The upper reservoir consists of a highly lobate, river dominated system that during sedimentation was prograding into shallow water from the east, with large differences in petrophysical characteristics and with a clear anisotropy. The lower reservoir was generated by sediments prograding from the north into more tidal dominated water which results in less horizontal heterogeneity. Each of these reservoirs consists of four 20 meters thick sub-zones without smooth transitions between them. These two synthetic 3 by 9 km laterally extending reservoirs were stacked with a 20 meters thick, low permeability zone in between, giving a total of 180 meters thick vertical extent. This is considered sufficiently thick to ensure that the seismic analysis is not entirely dominated by edge effects. The combined zone was tilted with a dip of 3.4 degrees dipping towards the west, see Figure 1.

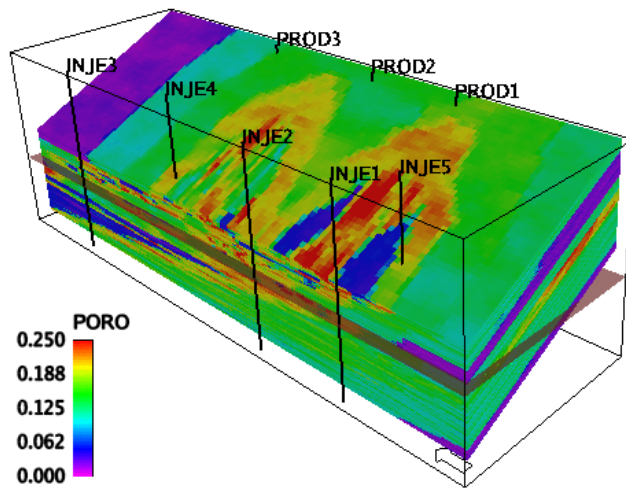


Figure 1. Porosity distribution in synthetic true reservoir is shown with wells and owc level. Reservoir covers 3 by 9 km and has constant thickness of 180 meters. Eastern edge of reservoir is at 1800 meters depth, western edge at 1980 meters, while owc is at 2020 meters. North is indicated by the arrow below the reservoir. Rows west of injectors 1-3 are not shown.

Due to the dipping structural constraints of the reservoir, the 5 vertical injectors were put close to the western edge, where the owc is close to the top of the structure. The 3 vertical producers were drilled near the crest at the east. Moreover, a thin (2 meters) high permeability thief-zone that runs from the southern edge across the reservoir from east to west was also added. It is located 20 meters below the top structure, hits the three southernmost wells, and terminates just before hitting also well INJE2. The thief zone replaces a high

heterogeneous anisotropic (east-west) region with mean horizontal permeability 180 mD (std. dev. 279 mD), with a smooth isotropic permeability field with mean 1003 mD (std. dev. 52 mD).

Flow simulation

The fluid flow was simulated using a commercial reservoir simulator (Schlumberger, 2001). One set of relative permeability and capillary pressure curves, based on typical curves from a North Sea field, was used for the entire reservoir (see Figure 2). Similarly, one set of PVT properties (B_w , B_o , B_g , water-, oil-, gas-viscosity, RS, density), based on the same North Sea field, was used. Datum and initial gas-oil contact was set to 1800 m and oil-water contact was set to 2020 m, reservoir pressure at datum was set to 285 Bars.

The 5 vertical injection wells (Figure 1) all inject at constant injection rate of 25000 m³ per day. The 3 vertical production wells all produce at constant bottom hole pressure BHP.

Saturations and pressure in the reservoir were saved for each grid block at time intervals of 200 days, and used for the subsequent seismic modeling.

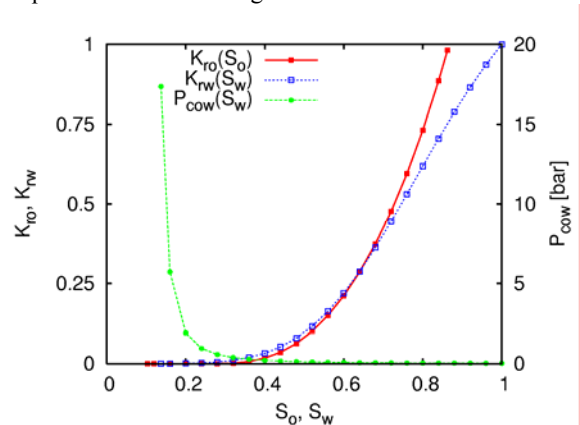


Figure 2. Saturation functions used in the synthetic reservoir. Red and blue curves are relative permeability of oil and water, $K_{ro}(S_o)$ and $K_{rw}(S_w)$, as functions of oil and water saturation, S_o and S_w , respectively. The green curve is capillary pressure curve of water as function of water saturation.

Simulator-to-seismics workflow

A workflow for predicting the elastic and seismic response to production is depicted in Figure 3. For each layer of the flow simulator model, the elastic response is predicted using a rock physics model calibrated for the specific target lithology and the effects to be modeled. Subsequently the elastic model is entered into the seismic modeling module to predict the appropriate seismic response.

A rock physics model provides the framework for converting the geological properties of a rock, both static and dynamic properties, into the elastic properties that determine the seismic response. The rock physics models are generally calibrated using the available data from a field, e.g. well logs and ultrasonic laboratory measurements. The workflow opens up for rock models ranging from simple empirical models, via hybrid poroelastic and scattering models for sands to complex anisotropic models for shales.

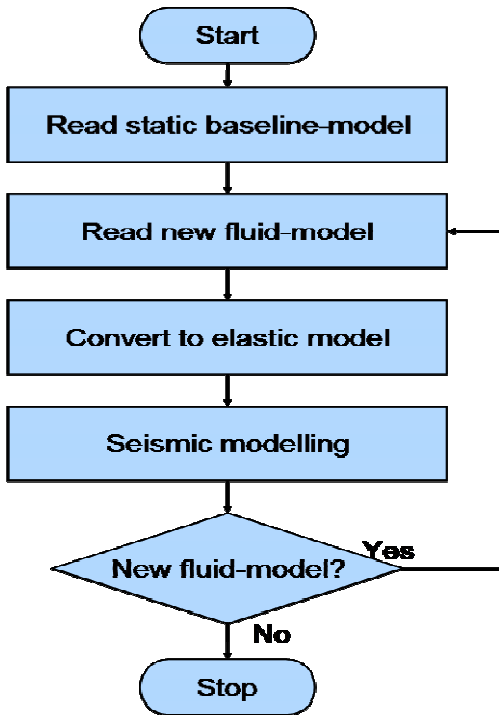


Figure 3. Forward modeling workflow from flow simulator to seismics.

The effect of production on elastic rock properties varies with the changes in fluid saturations and composition and physical conditions in the reservoir such as pore pressure and temperature. The strength of the production effects depend on both the lithology, the rock microstructure, the fluid properties and the saturation type, e.g. whether the fluid mixing is homogeneous or patchy should be considered (Johansen et al. 2002). In Figure 4 is the sensitivity to the oil saturation shown for a given porosity in one layer in the simulation model. The figure indicates that a significant oil-brine contact can be expected in the elastic and seismic responses, mainly due to the change in P-wave velocity.

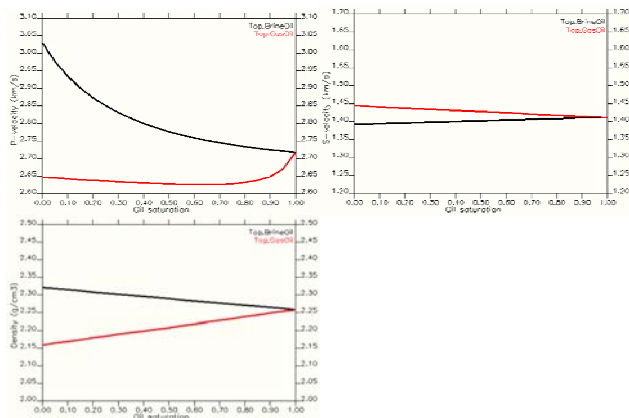


Figure 4. Predicted response in seismic velocities and density to changes in the oil saturation. The black line corresponds to a transition from brine to oil, whereas the red line corresponds to a transition from gas to oil.

The seismic modeling uses the “Simulated Prestack Local Imaging” (SimPLI) approach, a concept developed for efficient modeling the seismic response of complex hydrocarbon reservoirs (Lecomte et al., 2003 and Lecomte, 2004). SimPLI allows an interpreter to analyze the dynamic reservoir models in terms of seismic response, i.e. PSDM (Prestack Depth Migration) amplitudes, where the illumination and resolution properties from the survey and overburden are taken into account.

Figure 5 shows the oil saturation and corresponding elastic and seismic response from a line between INJE1 and PROD1 (see Figure 1) at both base and monitor times of the flow simulator model.

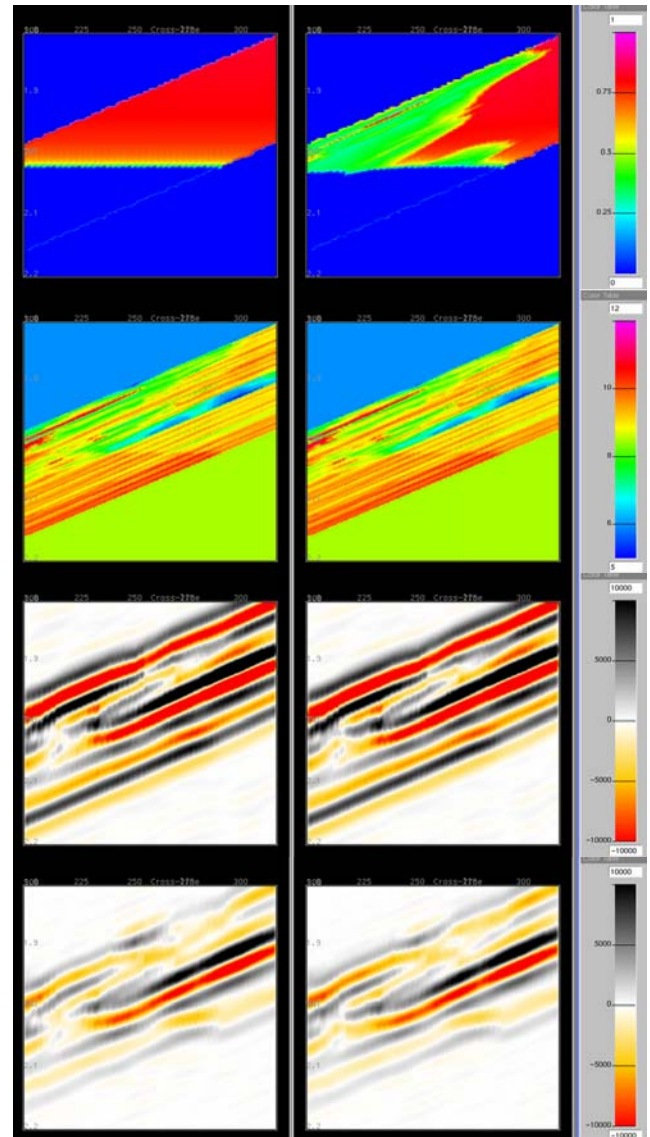


Figure 5. The results from the simulator-to-seismics workflow for a selected line. The left column contains the initial properties and the right column contains predicted properties after 800 days. From top to bottom are the oil saturation, the acoustic impedance, the zero-offset seismic response and the far offset seismic response.

As shown in the figure it may be difficult to identify the changes in the elastic and seismic response alone. Attempts to identify the locations and magnitudes of the differences are often made. Figure 6 shows the corresponding difference sections between the two data sets shown in Figure 5.

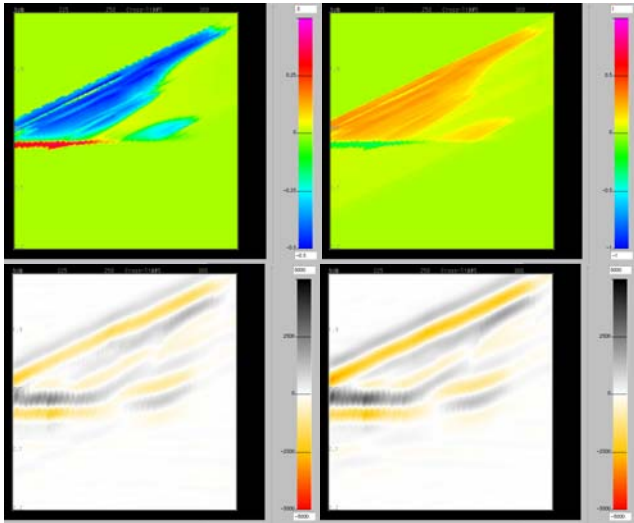


Figure 6. Difference sections from the simulator-to-seismics workflow for a selected line. Top row is the change in oil saturation (left) and P-impedance (right). Bottom row is the change in zero-offset response (left) and far offset response (right).

The figure shows how the drop in oil saturation corresponds to an increase in the acoustic impedance which causes the corresponding differences in seismic response.

Elastic seismic inversion

For the synthetic reservoir, the elastic and seismic modeling of the reservoir rock at a certain saturation and pressure situation also provide the exact elastic parameters (pressure velocity, V_p , shear velocity, V_s , and density) that corresponds to the seismic amplitude. These data will of course never be available on the full reservoir, but only at well locations, where logs may exist. In a non-synthetic, real case, the available data are therefore the seismic amplitudes on the reservoir, and logs at the wells. The well logs are natural to use in calibrating purposes, as those locations have both elastic and amplitude data.

The methodology of Bayesian inversion described in Buland et al. (2003) is used. The Bayesian approach defines the prior distribution and constrains this by data to form the posterior distribution. The prior model is defined by random fluctuations around a low frequent background model. The background model for the elastic parameters can not be deduced from the seismic amplitudes, but is based on smoothed well logs. First, a vertical moving average is done within each well. This averages the neighboring cells within 20 meters above and below the target depth. The rationale behind this smoothing is to remove heterogeneities that affect the seismic response. Then, a long ranged kriging is performed that populates the remaining reservoir with values based on the eight smoothed wells. Thereby a slowly varying

background model is generated that can contain also regional trends within the reservoir, and that corresponds to the well data, see Figure 7. The random fluctuations around this background are defined by correlations. The pointwise correlation between elastic parameters and the vertical correlation is estimated from the well logs. The lateral correlation range is assumed to be 1000 meters, but it is not possible to verify this from the well data since it is impossible to estimate this with such a low number of wells. The inversion methodology uses a linearized approach, where the seismic forward model is described as a convolution between a wavelet and seismic reflectivity. The link between seismic reflectivity and elastic parameters is approximated by a continuous version of the weak contrast approximation to Zoeppritz equation, (Stolt and Weglein, 1985). In the inversion angle stacks for 0, 5, 20 and 30 degrees are used. The inversion result is both an estimate and an updated correlation function describing typical fluctuations around the estimate.

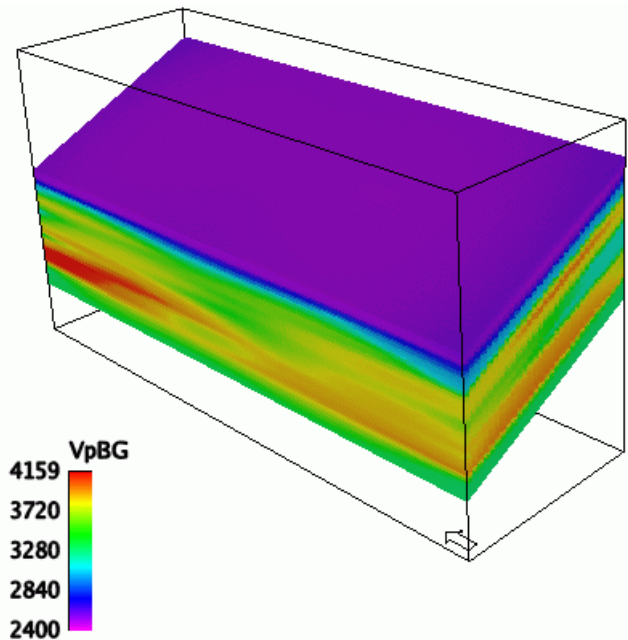


Figure 7. Background model for pressure velocity, V_p . The inversion also will consider locations above and below the actual reservoir due to the bandwidth of the wavelet. Therefore, background values are generated also above (lilac) and below (lower green part) the reservoir at study.

In Figure 8, the elastic parameters were plotted against the corresponding parameters used for generating the seismic amplitude to QC the inversion. The pressure velocity is shown at one of the wells, and at a high heterogeneous location far from the wells. It is seen that the main features are captured, but since the inversion is a prediction with limited band width, the small scale variation seen in the true data is not present.

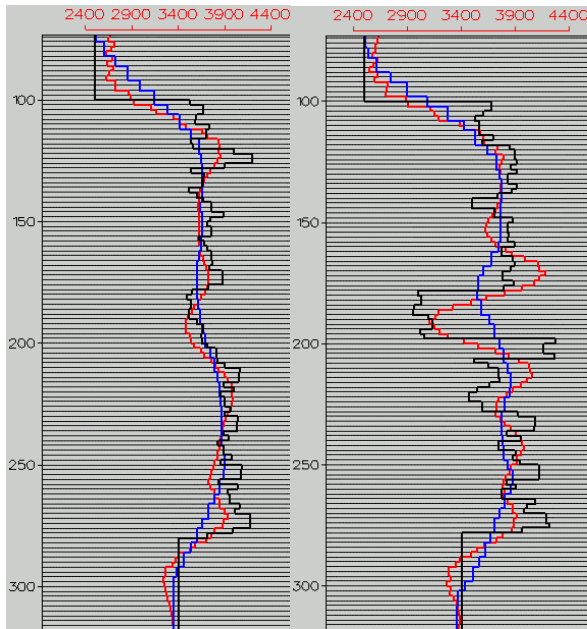


Figure 8. True Vp shown in black, inverted in red and the background Vp level shown in blue. The left picture shows the logs in well INJE2, and the right the logs along a vertical trace near the center of the reservoir in a high heterogeneous region. The y-axis indicates depth in meters.

Another QC procedure available since the true reservoir is known is to compare the elastic inversion with the corresponding true value based on the rock physics model. An example is to see where the true pressure velocity deviates much from the inverted. In Figure 9 this is shown at a region around a high deviance location near the bottom of the reservoir.

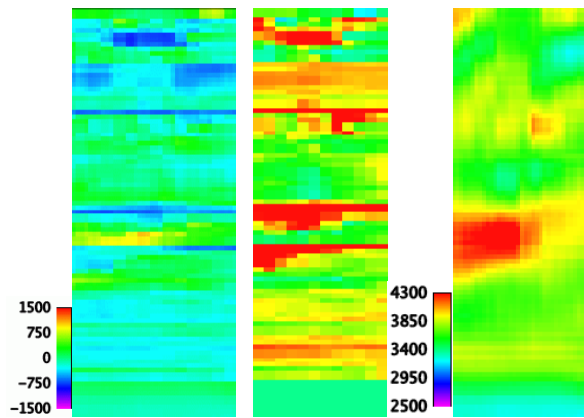


Figure 9. Difference between inverted and true Vp at a selected region before any production (left), true Vp (middle) and inverted Vp (right). Middle and right picture has mutual color legend.

It is apparent that high local error is occurring where there is high variability in the true Vp values. At the red spot in the center on the left picture the predicted inverted Vp value is about 1000 m/s higher than in the true Vp. Looking at the true velocity field, there is a high variability of very limited

thickness at that spot. Due to the bandwidth of the seismic inversion, that thin zone of less Vp cannot be found with confident with the inverted method. The right picture shows the inverted Vp, and as expected the fine details of the true Vp is averaged out as if it was used a moving average window over the true Vp field. After the inversion the well data was used to condition on the actual values of elastic parameters in the well, using a kriging procedure.

This affects a region around the wells determined by the updated correlation function.

Stochastic petrophysical simulation

To complete the workflow loop, new petrophysical realizations need to be simulated. For simplicity, their average, the predicted realization was chosen here, together with a conservative, naïve modeling approach. This means that only the well data and the inverted elastic parameters were used, no knowledge about the heterogeneous sedimentology (facies) was used; neither were any internal zonation information, although in an applied situation for a real field, this often is at least partly known. The predicted petrophysical realization was therefore simulated as belonging to one thick zone, and conditioned on well data and a seismic parameter.

Since the three inverted elastic parameters are highly correlated, it was decided to combine them into a new parameter that contains the necessary information about the petrophysical parameters to be simulated. This is done simply by performing a linear regression on the petrophysical and the elastic inverted parameters in the well. An optimal (within linear combinations) new parameter is thereby generated, that is suitable for cokriging with the petrophysical parameters. In Figure 10, the correspondence between the true and the predicted porosity using the new combined parameter is shown.

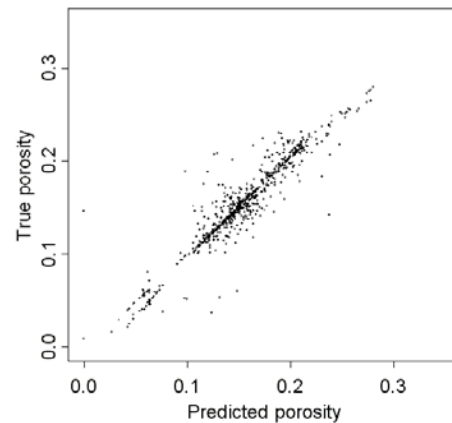


Figure 10. Correspondence between true porosity from well logs and the collocated predictions based on the elastic parameters.

The estimated correlation was 0.934 in the wells, whose magnitude is higher than the correlation of any of the elastic inversion parameters. These were -0.829, -0.771 and -0.916 for Vp, Vs and density respectively.

The permeability in the synthetic reservoir is significantly anisotropic, with direction that changes in the different sub-zones. The choice to not include that knowledge in the reservoir prediction model imply the same petrophysical

model for the permeability in x and y direction. It was however assumed that the permeabilities was lognormal, which is correct for the highest permeability facies. It is not correct with respect to the more shaly facies, but that is not considered crucial as the main flow do not occur there. The correspondence between the permeability along the x-direction (PERMX) is found in Figure 11.

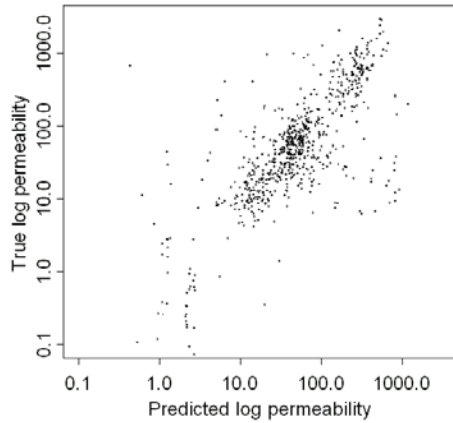


Figure 11. Correspondence between true x-directional permeability from well logs and the collocated predictions based on the elastic parameters is shown in a log-log plot.

As expected, the porosity is better correlated with the elastic inverted parameters than the permeability. Although the correlation is not as good as for the porosity, it still gives a fairly good conditioning parameter. The correlation between this combined seismic parameter and the true log-permeability in the wells is 0.756.

The approach used here is to first simulate porosity based on its corresponding linear combination of the elastic inversion parameters, and then under the stochastic model simulate the permeabilities conditioned on the well data and cokriged on both the previously simulated porosity field and the permeability derived linear combined seismic parameter. Limits were set to avoid negative values or unrealistically high values in all parameters.

For the stochastic model of the petrophysical parameters a set of input parameters need to be defined. All three permeability parameters (x-, y- and z-directions) were assumed to be lognormal while porosity and cell shale content (vsh) were assumed symmetric where the level was defined by the normal score transformation of the well data. The petrophysical distributions used in the Saigup study from which this synthetic reservoir has been generated, were based on representative real case reservoirs from the North Sea, implying that a realistic relationship between the different parameters should be achieved from the well data. No compactional, depositional or lateral trends were assumed. The amount of well data was not large enough to perform a proper variogram analysis, especially laterally, so variogram type and ranges had to be set. Vertically, a range fit gave around 20 meters for the different parameters, but with a large associated uncertainty. The variograms were all chosen to be spherical and with isotropic ranges of 2000 meters laterally and 20 meters vertically. These are long, but not unrealistic

settings compared to a real field example and therefore plausible as settings for a reservoir with as little known information as set out for here. Compared to the true reservoir, with six different facies associations and a separate thief zone, the ranges are too long.

The petrophysical simulation of the system produced a realization whose porosity distribution is shown in Figure 12.

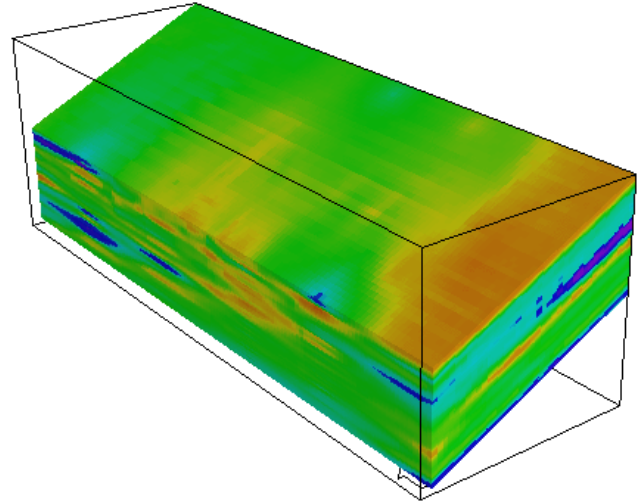


Figure 12. Predicted porosity realization of the reservoir conditioned on well data and cokriged with combined seismic parameter. Same color legend as in Figure 1.

Some features of the original synthetic reservoir are present, e.g. the east-west anisotropy is kept at the top of the reservoir. Also some of the low porosity (blue) regions correspond to the original, but they have less extent. Some of the high porosity lobes (red) locations also correspond. There seem to be less heterogeneity, but this is expected partly since this is a prediction, but also since the seismic data is band limited, a certain smoothing is natural. It is difficult to compare only by visual means. Even more important, it is the fluid flow that is affected by the petrophysical realization that is the target which should be compared with the flow of the original synthetic reservoir.

In the high permeability thief zone the deviancy between the true field and the simulated field was measured. The average difference was 839 mD with a standard deviation of 191 mD. In the corresponding layer above the difference was only 2.5 mD with a standard deviation of 212 mD. The predicted permeability in the thief zone corresponds e.g. better with the true values of the layer directly above than the true values of the thief zone. That average difference is 0.7 mD, with a standard deviation of 243 mD. It is obvious that the thief zone was not detected by the predicted petrophysical parameters based on the inverted elastic seismic parameters.

An interesting question is to what degree the relations between seismic parameters flow parameters can be extrapolated from the wells into the full reservoir. A measure for this is the pointwise correlation between the estimated parameters and the reservoir parameters. For the full field the correlation between the porosity and log permeability and the corresponding combined seismic parameters are 0.706 and 0.652 respectively. This is quite satisfactory. These

correlations cannot be directly compared with the well correlations (0.934 and 0.756) since the resolution in the combined seismic parameter decay away from the wells. The gap between the two correlations indicates the amount of variability in the seismic parameters that remains unresolved by the inversion.

The well data were not representative for the true petrophysical properties in the synthetic reservoir, especially for the x-directional permeability, which is the major parameter controlling the flow from the injectors at the west to the producers at the east. And as a result from this, the permeability level of the predicted reservoir becomes too low. This situation is unavoidable if the petrophysical parameters are conditioned only on biased well data.

Flow comparison of predicted and true reservoir

The most relevant domain for comparison between the predicted and true reservoirs is the flow domain, as this is the domain and scale where the physical flow in the reservoir is measured. Moreover, it is on this domain full-field flow simulations are subjected to be history-matched. Good flow predictions therefore improve the history-matching process, and serve as more accurate support for decisions regarding the depletion strategy of the reservoir. A flow simulation was therefore made on the predicted reservoir using identical conditions on the predicted petrophysical parameters as for the true synthetic reservoir. The oil and water productions in the three producers are found in Figure 13.

The thief-zone present in the original reservoir was not detected or honored in the inverted elastic parameters, and is therefore not present in the predicted petrophysical parameters. This fact can to a large extent explain the differences in well production rates between the original and predicted reservoirs at well PROD1. In the true reservoir, this producer is in direct contact with the thief zone, which is absent from the predicted reservoir. The effect of this difference is clearly visible as a time lag of about 2 years in the water break-through in the predicted vs. the true reservoir. In addition the predicted water production is much lower than in the true reservoir. Since the predicted reservoir misses the massive water breakthrough due to the thief zone, the oil production is also far too optimistic after the time of true water break-through (about 1 1/2 years). In wells PROD2 and PROD3, not directly in contact with the thief-zone, the water break-through is actually earlier in the predicted than in the true reservoir, but the difference in water production is less pronounced than for PROD1. The overall correspondence between predicted and true reservoir is much better for these two producers, both for water and for oil, although the oil production is underestimated in both cases. Well PROD2 is located in the middle of the high porosity, high permeability region of the reservoir. The oil production rate has a good correspondence in shape, but at a too low level. The generally lower permeability level in the predicted reservoir can explain the lower production. Above the owc, the cells have on average approximately half the horizontal permeability of the true reservoir. The last producer (PROD3) shows some similarity with the second. The exception is that now actually both the oil and water production rate decreases in the predicted reservoir. It is therefore not water that expels oil

here; it is a generally lower production. This can be explained by the lower permeability level in the reservoir.

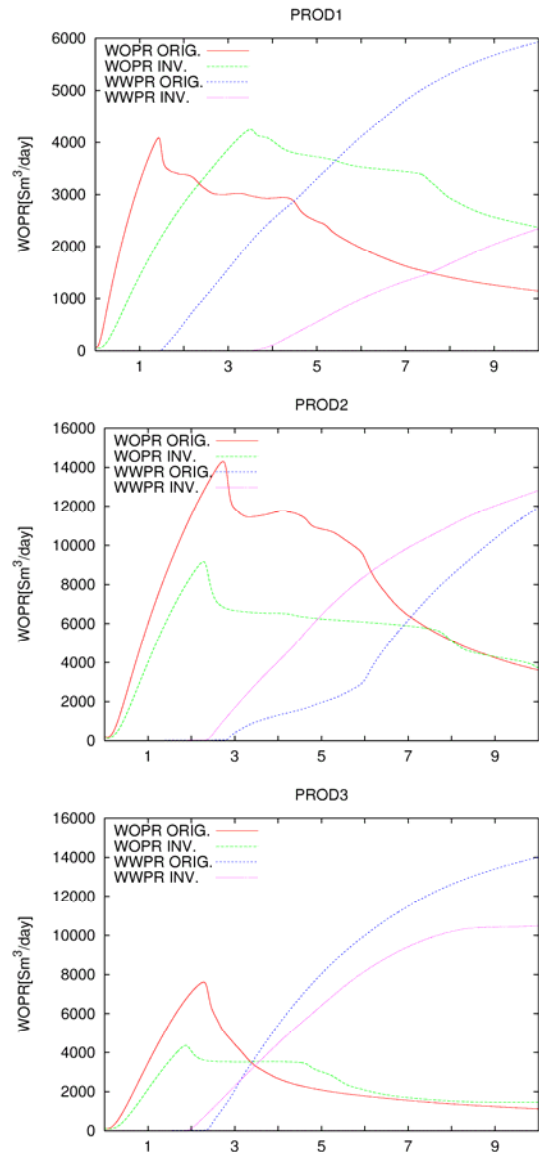


Figure 13. Well oil (WOPR) and water (WWPR) production rates in years after production start at the three producers. The rates are shown for both the true reservoir (ORIG) and the reservoir predicted from the inverted elastic parameters (INV).

The smoother, less heterogeneous petrophysical fields means less fingering. This should imply a reduced mobility in the reservoir and an increase in time to water breakthrough. For producers PROD2 and PROD3 the opposite occurs. The fingering effect thereby seems to have been neutralized by the effective increase in variogram range which ensures that the relatively high permeable paths that exist are large enough to connect the injectors and producers better than in the true reservoir.

It was to be expected that the predicted reservoir would deviate from the true in flow behavior. It is therefore natural to try to improve the predictions by using 4D seismic data.

4D seismic data

The seismic modeling was done on a series of time steps, in order to reflect the changes in the reservoir after the reservoir has been under production. These time steps are corresponding to the times of the monitor surveys for repeated time-lapse seismic data collections.

The first time-lapse seismic data set chosen were after 800 days of production, which is relatively early in the production life cycle. The forward seismic modeling procedure that was done for the initial situation were repeated, but subjected to the changes in saturation and pressure from the injection and production during these 800 days. The resulting seismic amplitude data from four angle gathers (0, 5, 20 and 30 degrees) will correspond to a real time-lapse seismic survey. These were subjected to inversion by the same method as the base case, and new inverted V_p , V_s and density predicted parameters were computed. Note that to avoid a new factor in the comparison; the inversion did not change the background model to account for the flow during the production period. That would theoretically improve the inversion parameters, but that would give an inversion with slightly altered boundary conditions as the base survey inversion. The motivation is not to optimize the elastic parameters V_p , V_s and density, but using these inverted parameters to assist finding realistic petrophysical parameters that are close to the true petrophysical properties of the synthetic reservoir.

The elastic inversion now provides V_p , V_s and density as before, but also the changes in these parameters since the base inversion. A natural question is whether or not it is possible to use these in an automatic matter in order to improve the seismically conditioned petrophysical parameters. To investigate this, a linear combination of the new inversion parameter and their changes since the base survey was made. The method was similar to the combined parameter generated from the base inversion, but adjusted for the fact that six parameters generally explain more than three does.

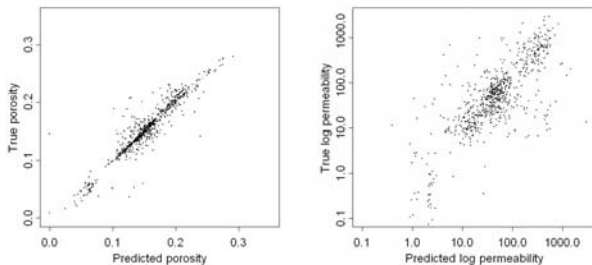


Figure 14. Correlation between true petrophysics and predictions conditioned on optimal linear seismic parameter for porosity (left), and x-directional log permeability (right) in all wells.

By comparing Figure 14 with the correlations found from the base inversion in Figure 10 and Figure 11, it is seen that the new data (the 4D differences) did not add any significance in this context. The estimated correlation adjusted for the number of parameters changed from 0.934 to 0.935, and the x-directional permeability changed from 0.756 to 0.766, quantifying the lack of extra information in the 4D data at the well locations.

However, 4D data can be utilized differently. The 4D data did not add more information in the well locations, but its

strength is instead to show the change in saturations along the flow paths between the wells. The difference parameters, e.g. between monitor and base time $\Delta V_p = V_p(t=800) - V_p(t=0)$ contain local information about the flow that indicates where the petrophysical parameters in the predicted reservoir are wrong.

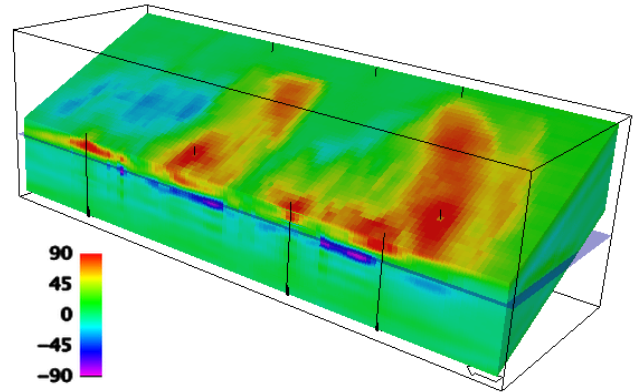


Figure 15. Difference in inverted V_p from monitor to base survey, with wells and owc level. Here, the uppermost shown layer is the thief zone. Rows west of injectors 1-3 not shown. Warm colors indicate a velocity increase; i.e. water replacing oil.

Figure 15 show that there is a relatively high positive change in the V_p in the thief zone layer. But it is not significantly higher in the thief zone part (southern) of that layer than the rest of that layer accounting for the injector locations. Close to the wells, the predicted permeability is high due to the conditioning. However, a large part of the area between the wells has permeability around 100 mD, while the true had around 1000 mD. The high V_p change observed is not compatible with those low permeabilities. This suggests an increase in the permeability level in the thief zone, but also in the zones adjacent to it, since the difference in V_p is high also there at low permeability parts of the predicted reservoir. It is however not directly deductable in which of the layers the permeability level should be increased the most, as the 4D data are on a coarser vertical scale. Moreover, the petrophysical properties in the layers adjacent to the thief zone have a high correspondence with each other and with the thief zone layer, as they all come from the same stratigraphical zone.

The anisotropic nature of the true reservoir is seen in ΔV_p and can be used to improve the predictions of new petrophysical parameters. This can be achieved by acknowledge that anisotropy in the variograms of the relevant petrophysical parameters.

Comparing 4D seismic with saturation data

Since the true reservoir is known here, a comparison between the 4D seismic data and the computed saturations for both the true and the predicted reservoir can be made. In Figure 16, the oil saturation is shown for the true and the predicted reservoir at the same time as the 4D data was taken from. The true reservoir clearly shows the thief zone as a region where the water has replaced oil along the southern part of the reservoir.

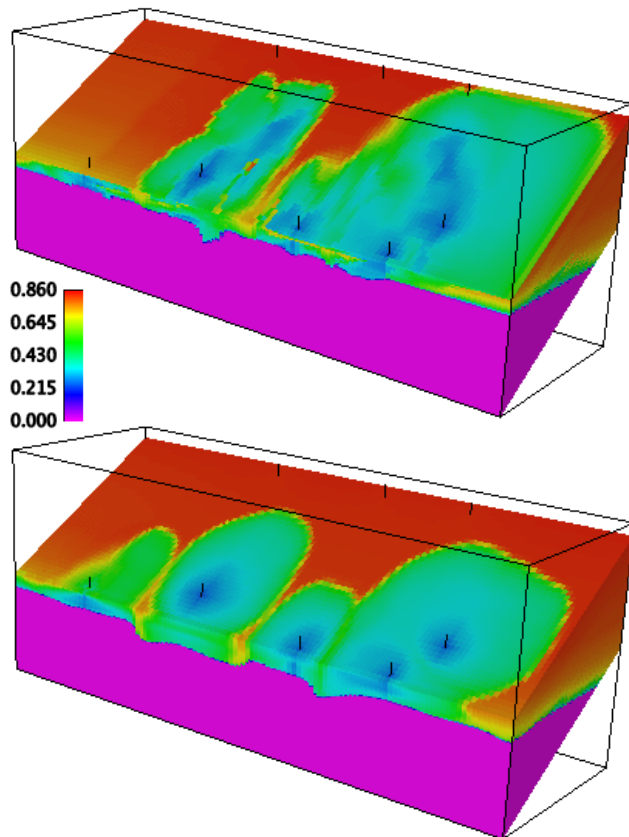


Figure 16. Oil saturation in true (upper) and predicted (lower) reservoir, shown from thief zone layer and below. Well paths are indicated in black.

This is less pronounced in the predicted reservoir. The anisotropic flow behavior is also recreated, but the predicted reservoir gives smoother water propagation, as expected. Comparing with Figure 15, the true reservoir shows good resemblance, confirming that the seismic modeling and inversion captures the changes in the reservoir in the 4D data. In the predicted reservoir, the water is further away from the producers, which means that the permeability in the reservoir should have been higher.

The situation for the layer below the thief zone is shown in Figure 17. The water propagation for the true reservoir shows a lobate shape, without the thief zone's wide extent, and the predicted reservoir is highly correlated with its adjacent upper layer in Figure 16. Again it shows too smooth water propagation compared with the true reservoir. Since there are two injectors in the southernmost lobe, the water propagation in the predicted reservoir is not unrealistic.

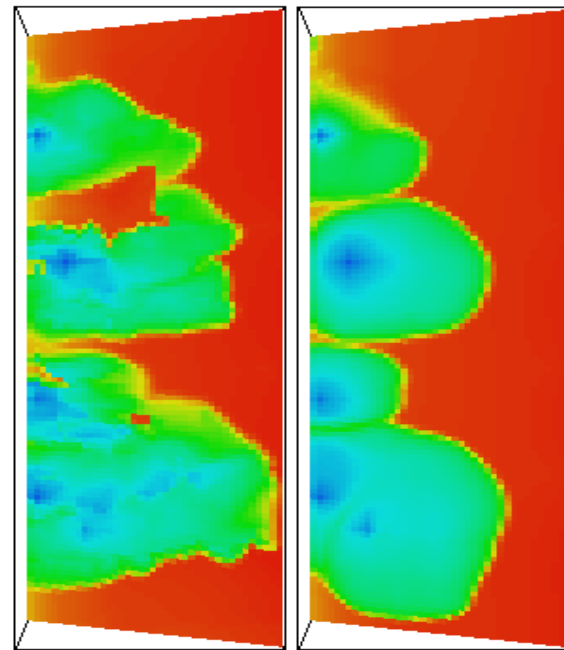


Figure 17. Oil saturation one level below thief zone for the true (left) and predicted (right) reservoir at time of monitor survey.

Updated stochastic modeling

The challenge in utilizing the 4D data (Figure 15) is to combine them with the observed mismatch in the wells and other data sources like the predicted saturations (lower part of Figure 16 and rightmost of Figure 17) in order to update, or regenerate the petrophysical properties to improve the match. The fact that ΔV_p is similar to the water propagation of the true reservoir is useful in regions where there has been a direct influence by the production. Outside this region, the ordinary elastic inverted seismic data must guide the reservoir characterization together with any other available data.

A 3D trend parameter for use in the petrophysical modeling was now created in order to try to improve the results. The idea was to use the most significant changes in oil saturation change (ΔS_o) from the predicted reservoir at time of monitor survey, and the corresponding 4D seismic data (used ΔV_p for simplicity here) to update the petrophysical modeling. Values of $|\Delta S_o| > 0.1$ and $|\Delta V_p| > 20$ m/s were chosen to be significant enough to carry relevant information. First a discrete parameter for both ΔS_o and ΔV_p was created. Then these were merged into one 3D discrete parameter where the value 1 means locations where $|\Delta V_p| > 20$ m/s, -1 means locations where $|\Delta S_o| > 0.1$, but where $|\Delta V_p| < 20$ m/s, and 0 means no significant information, see Figure 18. The idea was to have a positive value where high permeabilities could be assumed from the 4D seismic and saturation data from the initial prediction. Similarly, negative values in the 3D trend parameter would indicate where the permeability should decrease and a zero value where the data did not give any information about the permeability. Thereby, a discrete 3D trend parameter suited for use in the petrophysical modeling was achieved. A discrete parameter is a rough approach, and using the scale of the change in ΔS_o and ΔV_p would be a natural extension, not pursued here. Note that at the south edge

this new parameter has a region around the thief zone layer that incorporates the 4D seismic information about significant V_p change there. The region is between 2 and 5 layers thick, so the seismic data resolution is unable to pick the actual layer.

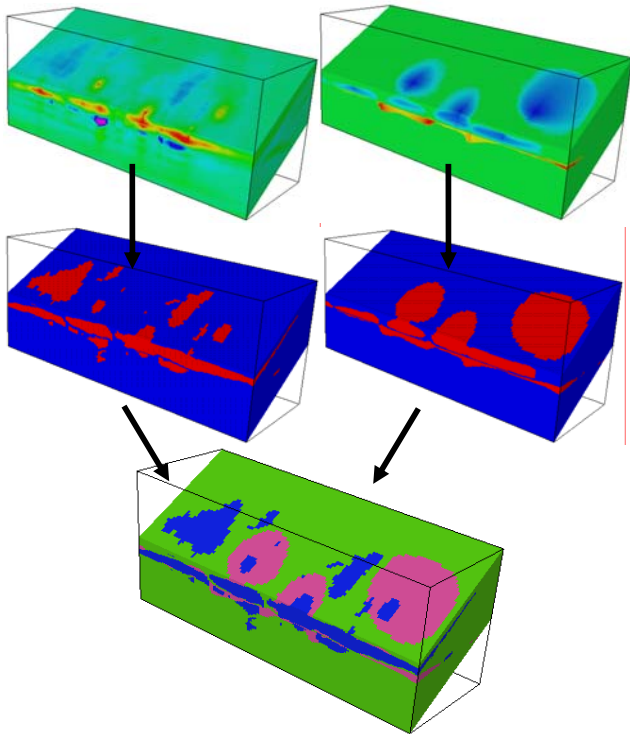


Figure 18. Generating a discrete 3D trend parameter from ΔV_p (left column) and ΔS_0 (right column). Cube is shown from upper layer and down. The lowermost trend parameter is blue for increasing and pink for decreasing permeability level, while green indicates no permeability change regions.

The petrophysical predictions were now rerun for PERMX and PERMY only, since there were indications to support a change in these. In addition to account for the new 3D trend, the cokriging with the existing porosity field was kept in order to preserve the relationship between porosity and permeability. The average permeability level was also increased by about half the difference between the true (152 mD) and predicted reservoir (72 mD) since the 4D data suggested higher mobility in the reservoir. Still, the average permeability (113 mD) is lower than in the true reservoir. Every other simulation parameter was kept as in the first prediction. The new predicted PERMX is shown in Figure 19 together with the true and the first prediction for comparison.

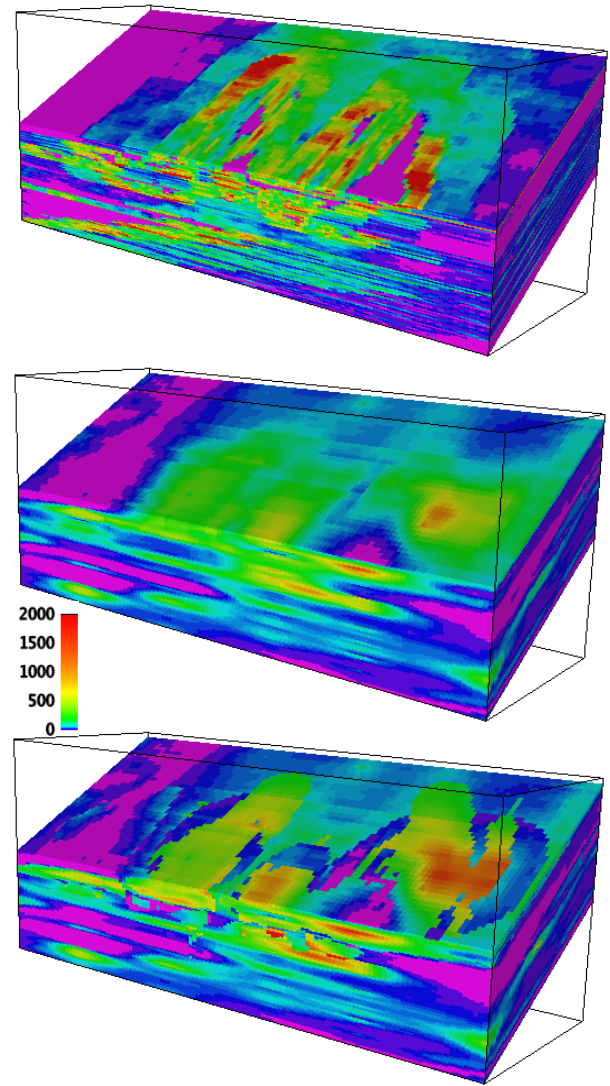


Figure 19. PERMX for true (upper), first predicted (middle) and new predicted with 3D trend parameter generated from 4D data (below). Reservoirs are shown without their upper 4 layers to ensure a representative image from within the reservoir.

The new permeability field became less smooth than the first prediction, in the regions where there was 4D information. Since the approach used a discrete parameter, the 3D trend parameter is clearly seen as a sharp transition that seems non-geologic, but this can easily be accounted for with a smoother 3D trend parameter.

The correlation with the true log permeability field for the full field decreased from 0.652 in the first prediction to 0.580 in the updated. Apparently, this has worsened the results, but correlation is a linear measure with limited strength in the non-linear flow domain. The new prediction needs to be checked through flow simulation of the reservoir.

Identical conditions for the flow simulations as previous simulations produced the results shown in Figure 20.

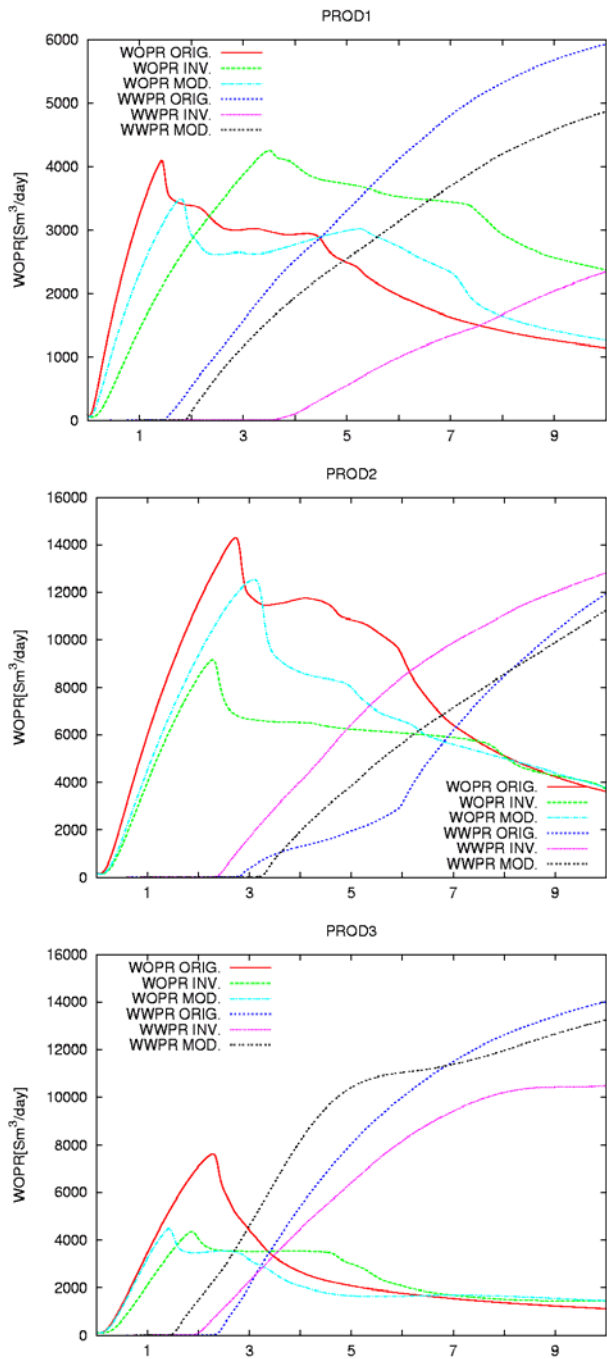


Figure 20. 4D modified (MOD) oil (WOPR) and water (WWPR) production rates compared with production from true (ORIG) and inverted elastic parameters conditioned (INV) reservoirs at all three producers.

Both oil and water production have improved significantly in well PROD1, located within the thief zone. The production is still too low, but given the fact that the permeabilities are lower in the new prediction compared to the true reservoir, this is not surprising. Well PROD2 also shows a strong improvement in its production of oil and water. The oil production is on a too low level, but the water production is much closer to the true than the first prediction. The last well,

PROD3, does not show the improvements as the other wells. This well is located where there were small changes in the 4D data, and had therefore not been subjected to much updating in the modified prediction. 4D seismic data for a later monitor time would increase the effects near this well, but whether that brings the production closer to the truth is not yet tested.

Conclusions

Utilizing 4D seismic data has been investigated on a realistic synthetic reservoir. The workflow has attempted to mimic a realistic reservoir modeling using seismic data. Forward seismic modeling was done on the synthetic reservoir at two time steps in order to obtain realistic amplitude data as in a real 4D study. Elastic inversion parameters were generated for the base time, and a linear combination of these was used as a conditioning parameter for predicting petrophysical properties. A full flow simulation of the predicted reservoir revealed a mismatch in both production and 4D seismic data obtained by inverting the seismic amplitude data to elastic parameters on the monitor time. This called for a modification of the petrophysical properties.

Significant improvements were made although the updated petrophysical parameters were generated in a naive way. One significant difference compared with the true reservoir is that the sedimentological modeling was omitted, so petrophysical parameters were not generated within different facies. Then, predictions were used implying the parameters becoming too smooth compared to a realistic reservoir. Using a suite of simulated petrophysical parameters would enhance this heterogeneity. Although the 3D trend parameter was simple and discrete, the procedure was able to detect some regions where an updated improved flow simulation results. This was achieved on the modified prediction accounting for the 4D seismic derived trend parameter. The procedure is suitable for repeated 4D seismic data since the modifications of the petrophysical properties are collocated with the changes in 4D seismic data and saturations. Thereby the updating is local since it did not affect regions without significant changes in saturation or inverted elastic parameters.

The thief zone was not distinguishable in one elastic inverted parameter, but with the 4D information, the impact of the zone was seen in the correct part of the reservoir, although not as narrowly distributed as in the true reservoir.

The information content in the 4D seismic data was confirmed by recognizing good comparison between the 4D data with the saturation results from the flow simulation of the synthetic reservoir.

The 4D-modified reservoir with updated saturations at monitor time can be subjected to a new seismic modeling and subsequent inversion. A workflow suitable for history-matching can be established by evaluating new realizations according to their 4D seismic data and saturation match. Modifications of the reservoir characterization that decrease the difference will be accepted, until an acceptable convergence has been reached under this framework. For such a history-matching setting, the petrophysical realizations should be stochastic simulations to ensure a larger span of realizations with realistic heterogeneity.

Acknowledgements

The study was done in a project sponsored by the Norwegian Research Council. The authors wish to thank them, and also our colleagues Øyvind Dugstad, Tom Pedersen and Petter Abrahamsen. They have all contributed constructively in this project.

References

1. Skorstad, A. *et al.*: "Sensitivity of oil production to petrophysical heterogeneities". Proceedings of the Seventh International Geostatistics Congress, Banff, Alberta, Canada. Kluwer (2005).
2. Schlumberger. "Eclipse Technical Description 2001A" (2001).
3. Johansen, T. A. *et al.*: "An approach to combined rock physics and seismic modelling of fluid substitution effects", *Geophysical Prospecting*, 50, 119, 2002.
4. Lecomte, I. *et al.*: "Simulated Prestack Local Imaging: a robust and efficient interpretation tool to control illumination, resolution, and time-lapse properties of reservoirs", Expanding Abstracts, presented at the 73rd SEG Annual Meeting, Dallas, RCT 7.2, Oct. 26-31, 2003.
5. Lecomte, I.: "Simulating Prestack Depth Migrated Sections", extended abstract P071, presented at the EAGE 66th Conference & Exhibition, Paris, June 7-10, 2004.
6. Buland, A., *et al.*: "Rapid spatially coupled AVO inversion in the Fourier domain", *Geophysics*, VOL.68, NO.3 (2003) 824.
7. Stolt, R. H., and Weglein A. B.: "Migration and inversion of seismic data", *Geophysics*, 50 (1985) 2458.